Original Article
Costunolide suppresses melanoma growth via the AKT/mTOR pathway *in vitro* and *in vivo*

Hai Huang[1*], Junkoo Yi[2*], Song Park[4,5], Haibo Zhang[1], Eungyung Kim[1], Sijun Park[3], Wookbong Kwon[3,4], Soyoung Jang[3], Xiujuan Zhang[6], Hanyong Chen[7], Seong-Kyoon Choi[4,8], Sung-hyun Kim[9], Kangddong Liu[10], Zigang Dong[10], Mee-Hyun Lee[11], Zaeyoung Ryoo[3], Myoung Ok Kim[1]

[1]Department of Animal Science and Biotechnology, Kyungpook National University, Sangju-si, Gyeongsang buk-do 37224, Republic of Korea; [2]Gyeongbuk Livestock Research Institute, Yeongju 36052, South Korea; [3]Shool of Life Science, Kyungpook National University, Daegu, Republic of Korea; [4]Core Protein Resources Center, DGIST, Daegu, Republic of Korea; [5]Department of Brian and Cognitive Sciences, DGIST, Daegu, Republic of Korea; [6]Department of Pulmonary and Critical Care Medicine, Huashan Hospital, Fudan University, Shanghai 200040, China; [7]The Hormel Institute, University of Minnesota, Austin, Minnesota, USA; [8]Division of Biotechnology, DGIST, Daegu, Republic of Korea; [9]Department of Bio-Medical Analysis, Korea Polytechnic College, Chungnam, Korea; [10]Basic Medical College, Zhengzhou University Zhengzhou, Zhengzhou, Henan, China; [11]College of Korean Medicine, Dongshin University, Naju, Jeollanamdo 58245, Republic of Korea. *Equal contributors.

Abstract: Melanoma is the most common type of skin cancer and its incidence is rapidly increasing. AKT, and its related signaling pathways, are highly activated in many cancers including lung, colon, and esophageal cancers. Costunolide (CTD) is a sesquiterpene lactone that has been reported to possess neuroprotective, anti-inflammatory, and anti-cancer properties. However, the target and mechanism underlying its efficacy in melanoma have not been identified. In this study, we elucidated the mechanism behind the anti-cancer effect of CTD in melanoma *in vitro* and *in vivo* by identifying CTD as an AKT inhibitor. We first verified that p-AKT and AKT are highly expressed in melanoma patient tissues and cell lines. CTD significantly inhibited the proliferation, migration, and invasion of melanoma cells including SK-MEL-5, SK-MEL-28, and A375 that are overexpressed p-AKT and AKT proteins. We investigated the mechanism of CTD using a computational docking modeling, pull-down, and site directed mutagenesis assay. CTD directly bound to AKT thereby arresting cell cycle at the G1 phase, and inducing the apoptosis of melanoma cells. In addition, CTD regulated the G1 phase and apoptosis biomarkers, and inhibited the expression of AKT/mTOR/GSK3b/p70S6K/4EBP cascade proteins. After reducing AKT expression in melanoma cells, cell growth was significantly decreased and CTD did not showed further inhibitory effects. Furthermore, CTD administration suppressed tumor growth and weight in cell-derived xenograft mice models *in vivo* without body weight loss and inhibited the expression of Ki-67, p-AKT, and p70S6K in tumor tissues. In summary, our study implied that CTD inhibited melanoma progression *in vitro* and *in vivo*. In this study, we reported that CTD could affect melanoma growth by targeting AKT. Therefore, CTD has considerable potential as a drug for melanoma therapy.

Keywords: Costunolide, melanoma, AKT/mTOR pathway, proliferation, xenograft models

Introduction

The high mortality and poor prognosis of melanomas lead to a low five years survival rate [1, 2] for these patients, despite the deployment of targeted therapies. To date, surgery is still the critical treatment for malignant melanoma. Drugs such as PD-1, encorafenib, binimetinib, and CDk4/6 inhibitors, are commonly used to treat melanomas either alone or in combination [3-5]. The benefits of tyrosine kinase inhibitors, immunomodulatory therapies [6], and traditional chemotherapy [7] have effectively improved the overall survival of patients with melanoma. Nevertheless, more than 50% of the patients with melanoma are unresponsive to immunotherapeutic agents, such as BRAF, KIT, and MEK inhibitors [8-11]. Furthermore, melanoma pathogenesis involves numerous signaling pathways related to tumor growth and

metastasis [12]. Therefore, finding new inhibitors with low toxicity and high specificity is a high priority.

The signaling pathway of MAPK (mitogen-activated protein kinase) plays a significant role in melanoma research. However, previous studies reported that activation rates of BRAF and NRAS variations were increased in benign nevi with minimal malignant potential [13, 14]. Moreover, several tumors or cell lines that generate secondary resistance to BRAF inhibitors continued to proliferate and survive, although MAPK signaling continued to be inhibited [15, 16]. Thus, activation of the MAPK signaling pathway alone is insufficient to decipher the pathogenesis of melanoma. Additionally, the PI3K-AKT pathway can be activated along with MAPK signaling activation in melanomas. Segrelles. et al. (2002) reported that the AKT-dependent signaling pathway and MAPK signaling played an important role in early and later stages of skin carcinogenesis, respectively [17]. Thus, these two pathways represent fundamental mechanisms in melanoma progression.

Deregulation of AKT has been reported in several cancers and is associated with biological processes including cell proliferation, survival, apoptosis, and transcription. PI3K/AKT/mTOR and NF-κB pathway activation or the phosphatase tensin homolog (PTEN) or cyclin-dependent kinase inhibitor 2A (CDKN2A) damage contribute to the overall stimulation of proliferation and growth of melanoma cells [18]. Previous studies have revealed that the active form of phospho-AKT (p-AKT) was high expressed in primary melanoma tumors when compared with normal adjacent tissue. These findings contribute to a reciprocal 5-year survival rate in human metastatic melanoma [19]. In combination with the downstream target protein mTOR, the aberrant expression of AKT1 lead to highly metastatic melanomas. These melanomas result in 67% and 17% in lung and brain metastases of BRAFV600E/Cdkn2aNull mice, respectively. Furthermore, mutant AKT1 and AKT3 expression has been found to accelerate metastases in melanoma and breast cancer cells, respectively [20-22]. This suggests that AKT is a key factor in melanoma metastasis. Moreover, recent studies showed that p-AKT can rebound under BRAF inhibitor therapy alone or together with MEK inhibitor therapy

[23]. PI3K-AKT signaling inhibition showed a potential for enhancing or prolonging the anti-tumor effect of BRAF inhibitors [24, 25] in melanoma brain metastases [26]. Therefore, targeting AKT can compensate for the disadvantage of the BRAF inhibitors, further confirming AKT as a crucial therapeutic target in melanoma.

Recently, the pharmacological research methods have been developed to examine inhibitors targeting multiple components of the PI3K-AKT pathway, including PI3K inhibitors, duple PI3K/mammalian target of rapamycin pathway (mTOR) inhibitors, mTORC1 inhibitors, dual mTORC1/mTORC2 inhibitors, and AKT inhibitors [27]. Several of these inhibitors were extracted from natural compounds. In this study, we investigated the natural compound costunolide (CTD) (Supplementary Figure 1A) that possesses strong effects against growth in vitro and in vivo in colon, breast, and prostate cancer [28-31]. However, its pharmacologic function in melanoma has not been evaluated. Here we explored the potential inhibition of AKT pathway activity in melanoma cells in response to CTD treatment. We also investigated the anti-cancer effects of CTD against melanoma in vitro and xenograft growth in vivo. Our findings indicated that CTD is a novel potential AKT inhibitor that can attenuate skin carcinoma through AKT pathway, which therefore contribute to melanoma treatment in future.

Materials and methods

Melanoma tissue microarray

A total of 79 pairs of melanoma and adjacent tissue samples were collected from patients ages 13 to 77 years old at the point of surgery from Huashan Hospital of Fudan University in 2019. The patients had not received chemotherapy or radiotherapy. The paraffin-embedded section of tumor samples were provided by the Service Bio Company (Shanghai, China). The involvement of human subjects in this study was approved by the Research Ethics Committee of Huashan Hospital of Fudan University, and written informed consent have been obtained from all patients.

Chemicals and reagents

Costunolide (CAS: 551-21-9) was provided by Jonk Biological Technology Co. Ltd (Wuhan,

China) and had a purity ≥ 97% from HPLC and NMR analysis. Media (DMEM and MEM) were obtained from Gibco (Grand Island, NY, USA). MTT (3-(4,5-dimethylthiazol-2-yl)-2,5-diphenyl-tetrazolium bromide were obtained from Sigma-Aldrich. Primary antibodies tests were preformed in this project including phosphorylated of AKT, GSK3β (Ser 9), mTOR (Ser2448), p70s6k and 4EBP1, MEK, ERK, and the corresponding total antibodies. p53, cleaved caspase 3, Bax, cyclinD1, CDK4, and CDK6 were purchased from Cell Signaling Technology (Beverly, MA). Bcl-2 and antibodies to detect β-actin were acquired from Santa Cruz Biotechnology (Santa Cruz, CA).

Cell culture

Three human melanoma cell lines, SK-MEL5, SK-MEL-28, and A375, were obtained from the Korea Cell Line Bank (Seoul, Korea) and were cytogenetically tested and authenticated. Cells were maintained in MEM and DMEM that supplemented with 1% penicillin-streptomycin (100 units/mL) and 10% fetal bovine serum (Gibco), respectively. In addition, the human epidermal keratinocyte cell line used in this study was HaCaT (Mice Model Lab of Kyungpook National University Life Science). All cells were cultivated in standard incubators at 37°C with 5% CO_2. All cells were maintained in the culture for a maximum of 10 generations after thaw.

Cell viability assay

Well-conditioned cells were plated in 96-well plates (5×10^3 cells/well for HaCaT; 4×10^3 cells/well for SK-MEL-5 and SK-MEL-28; and 2×10^3 cells/well for A375), and then treated with DMSO (Sigma-Aldrich Co. LLC) and different concentrations of CTD (1.25, 2.5, 5 µM). Cell proliferation was measured every 24 h for 4 days by MTT assay. For soft agar colony formation assay, cancer cells (8×10^3 cells/well) were seeded in triplicate in 1 mL of cell culture medium with 2 mM glutamine, 5 µg/mL gentamycin, and 0.3% soft agar. The mixture was layered onto 0.5% solidified agar in cell culture medium in six-well plates. 2-3 weeks later, cells were photographed with a microscope and the number of colonies were counted using the Image-Pro Plus software (v.6.1) program (Media Cybernetics, Rockville, MD).

Cell cycle and apoptosis analysis

Cells were plated into 60-mm dishes (2.0×10^5 cells) for 24 h, and exposed to different concentration of CTD or DMSO for another 24 h before harvest. Before cell cycle analysis, cells were fixed in 70% ethanol at -20°C, and then re-suspended cell using 0.6% Triton X-100 buffer after being washed with PBS. The cells were incubated with RNaseA (200 µg/mL) for 30 min at room temperature. For apoptosis, cells were co-stained using annexin V and propidium iodide (10 µg/mL). After staining, the cell cycle distribution and apoptosis were analyzed using BD FACS Calibur flow cytometer (BD Biosciences, San Jose, CA, USA).

Migration and invasion assay in vitro

Transwell chambers (8-µm pore size; Costar, BD Biosciences, USA) were used in the *in vitro* migration and invasion assay, which was carried out following previously described methods [32]. In brief, cells (1×10^5) were re-suspended using DMEM without FBS and seeded in the upper chamber. The lower chamber was cultured in complete medium, after 24 h a different dose of CTD was administered. After another 24 h the medium was discarded, fixed in 4% formaldehyde, made permeable with 100% methanol, and stained with 0.5% crystal violet. The upper compartment cells were removed with a cotton swab and photographed with a microscope. In the invasion assay the transwell insert membrane was coated with matrigel while it was uncoated in the cell migration assay. For the scratch wound healing assay, cells were seeded into 6-well plates for 24 h, and cell monolayers were scratched using a sterile pipette tip. Then the cells were washed with PBS, treated with CTD for 24 h, and photographed. The data was analyzed using Image-Pro Plus software (v.6.1).

Computer docking model

Schrödinger Suite2019 was used for silico docking to confirm binding and communication of CTD with AKT. The crystal structures of AKT1 and AKT2 were derived from the protein data bank [33], and standard protein preparation protocols were followed. Hydrogen atoms were imported when the pH was 7 and all water molecules were protein preparation. The ATP-binding site-based receptor grid of AKT was generated for research docking. The CTD compound was prepared for docking using default parameters from the LigPrep program. The docking of CTD with AKT1 and AKT2 was accomplished using default parameters under

extra precision (XP) mode in the Glide program. This enabled the presentation of the best docking structure.

Western blot analysis

Melanoma cells were lysed and protein expression analyzed by western blotting following previously described methods [34].

Binding analysis using CNBr-CTD-conjugated beads

CTD-sepharose 4B beads and vehicle-sepharose 4B beads were prepared according to the manufacturer's protocol (GE Healthcare Bio-Science, Uppsala, Sweden). Cell lysates (500 μg) were introduced to CTD-sepharose 4B (or sepharose 4B only as a control) beads in a reaction buffer (50 mM pH = 7.5 Tris-HCl, 5 mM EDTA, 150 mM NaCl, 1 mM dithiothreitol, 0.05% NP-40, 2 mg/ml bovine serum albumin 20 × protease inhibitor). After incubation overnight with rotation at 4°C, the beads were washed three times with buffer (50 mM Tris-HCl; pH 7.5, 150 mM NaCl, 5 mM EDTA, 1 mM dithiothreitol, 0.01% NP-40, and 0.2 mM PMSF). Finally, the AKT binding was visualized by immunoblotting.

Site directed mutagenesis by PCR

Given that the mutant site of an ALA-to-Pro (*GCC > CCC*) was analyzed. An EZchange™ Site directed mutagenesis kit (enzynomics, KOREA) for Site Directed mutagenesis assay were conducted to investigate the alanine (ALA) of AKT as a binding site of CTD. Plasmids were isolated from the resulting colonies and screened for the desired modifications. Finally, the transformants for the desired mutations were screened using sequencing as appropriate (GenoTech Corp, Korea). The plasmids of AKT mutant were transfected into 293T cells using FuGENNE HD Transfection Reagent (Promega) and confirmed by pull-down assay.

Lentiviral construction and infection

For preparing the Akt1/2 knock down cells in melanoma the lentiviral expression vector of pLKO.1-mock, shAKT1 and shAKT2 were transfected into HEK293T cell with packaging vectors pMD2.0G and psPAX using the FuGENNE HD Transfection Reagent (Promega) following

the manufacturer's protocols. 48 h later, the viral particles were collected through filtration using a 0.45-μm filter and infected the cultured melanoma cells together with 8 mg/ml polybrene (Millipore, Billerica, MA) for 36 h. Then the stable cells were selected using 1 μg/ml puromycin and used for subsequent experiments. For AKT overexpression, the plasmids of pUSE-CA-AKT1 and pUSE-CA-AKT2 were transfected into melanoma cells by FuGENE HD Transfection Reagent. Concurrently mock plasmids were transfected into a control group. The stable cells were selected using 1 μg/ml G418 for 1 week. The selected cells were used for subsequent experiments.

In vivo analysis

Six-weeks-old nude mice were obtained from Charles River and were maintained in a specialized environment for 1 week before *in vivo* experiments. The study of animal experiments was approved by the Ethics Research Committee of Kyungpook National University (Dae-gu, South Korea). SK-MEL-5 cells (5×10^6 in 200 mL PBS) were subcutaneously injected into the right hind flank of three groups of mice (n = 8). After the tumor volume reached 100 mm^3 the mice were randomly divided into three groups and treated with the vehicle or 2 different doses of CTD (5 mg/kg and 7.5 mg/kg). CTD was administered intraperitoneally once every two days for 4 weeks. Body weight was recorded twice per week. The tumor volume calculation formula was length × width × depth × 0.52. Tumors were weighed, and frozen in liquid nitrogen or fixed in 10% formalin and embedded in paraffin after mice were euthanized and tumors extracted.

Immunohistochemistry analysis

The melanoma, tissue staining of immunohistochemistry was examined as previously described [35]. Briefly, after antigen exposure tissues were prepared by boiling the samples in sodium citrate buffer for 10 min. Then the samples were exposed to 3% H_2O_2 for 10 min and blocked with 5% BSA. Slides were incubated with specific primary antibodies at 4°C in a humidified chamber overnight. The slides were then incubated with secondary antibody for 30 min at room temperature. Slides were stained using 3,3'-diaminobenzidine and finally coun-

terstained with hematoxylin. At last, the sections were photographed and analyzed using the Image-Pro Plus software (v.6.1) program. The expression of the indicated proteins was quantified based on the percentage of positive cells.

Statistical analysis

All quantitative results were expressed as mean values ± SD. Significant differences were compared using two-tailed independent sample *t*-test between groups, and *p*-values of <0.05 were considered to be statistically significant.

Results

AKT is highly expressed in melanoma cells and reciprocally associated with patient survival

To examine the expression of AKT in melanoma patients. Melanoma microarray was conducted and results revealed that phosphorylated and total AKT were dramatically upregulated in cancer tissues, compared with adjacent tissues (**Figure 1A**, **1B**). This is consistent with results where AKT expression was significantly amplified at the mRNA level in melanoma patient tissues, compared with normal tissues in The Cancer Genome Atlas database (**Figure 1C**) (http://gepia.cancer-pk u.cn/index.html). Moreover, patients with high AKT expression had slightly lower survival rates than those with low AKT expression (P = 0.048, **Figure 1D**). (http://gepia.cancer-pku.cn/). AKT expression in cultured melanoma cells was also investigated by western blot assay and results showed that the expression of AKT in melanoma was much higher than in HaCaT (**Figure 1E**). These results indicate that AKT may be a potential target in melanoma treatment.

AKT is a potential direct target of CTD

Our previous results revealed that CTD targeting AKT directly independent of p53. Hence, to further determine the interaction between CTD and AKT a computer docking model was conducted to predict the communication between CTD and AKT1/2. Results of the docking model showed that CTD formed hydrogen bonds at Ala230 in the backbone of AKT1 (**Figure 2A**, upper panel) and at Ala232 of AKT2 (**Figure 2A**, lower panel), respectively. These results sug-

gest that CTD binds to AKT1/2 with a strong affinity. Moreover, the *ex vivo* pull-down assay also revealed that sepharose 4B beads conjugated with CTD, but not sepharose 4B beads alone, bound with AKT in melanoma cell lysates, suggesting CTD significantly binds with AKT (**Figure 2B**). To confirm that ALA is the binding site of CTD, we then conducted an *ex vivo* pull-down assay using a 293T cell lysate after transfecting mutant plasmids through direct site-mutagenesis. The results revealed that CTD bound less with mutant AKT, compared with the positive (overexpression AKT1/2) and negative (mock) groups. The results indicated that the ALA site of the AKT is a target binding site of CTD (**Figure 2C**).

CTD suppresses proliferation of melanoma cell, induces cell cycle arrest, and apoptosis

To estimate the threshold value between a therapeutic dose and toxic dose. We first determined the outcome of CTD on the growth of healthy HaCaT skin cells through MTT assay (Supplementary Figure 1B). Results suggested that there is no toxicity of CTD on melanoma from 1.25~5 µM. Moreover, cell proliferation was suppressed in a time- and dose-dependent fashion after CTD treatment on melanoma cells (**Figure 3A**). Through detailed statistical analyses (Supplementary Figure 1C), the dose of CTD ranging from 0 to 5 µM was considered as optimal. In addition, CTD attenuated the colony formation of melanoma cells by anchorage-independent growth assay (**Figure 3B**). This manifest not only in clone size, but also in quantity of colony formation, compared with DMSO-treated group (Supplementary Figure 1D).

In addition, flow cytometry was conducted to analyze the relationship between cell proliferation and cell cycle or apoptosis under the CTD treatment. The results showed that the incubation of melanoma cells with CTD for 24 h lead to cell cycle arrest at the G1 phase. The results matched the reduced expression of cyclinD, CDK4, and CDK6, as representative markers of the cell cycle at the G1 phase (**Figure 3C**, **3D**, Supplementary Figure 1E). Furthermore, we also found the apoptosis was triggered under CTD treatment (**Figure 3E**, Supplementary Figure 1F). To confirm the results, we examined total-cell lysates treated with various doses of
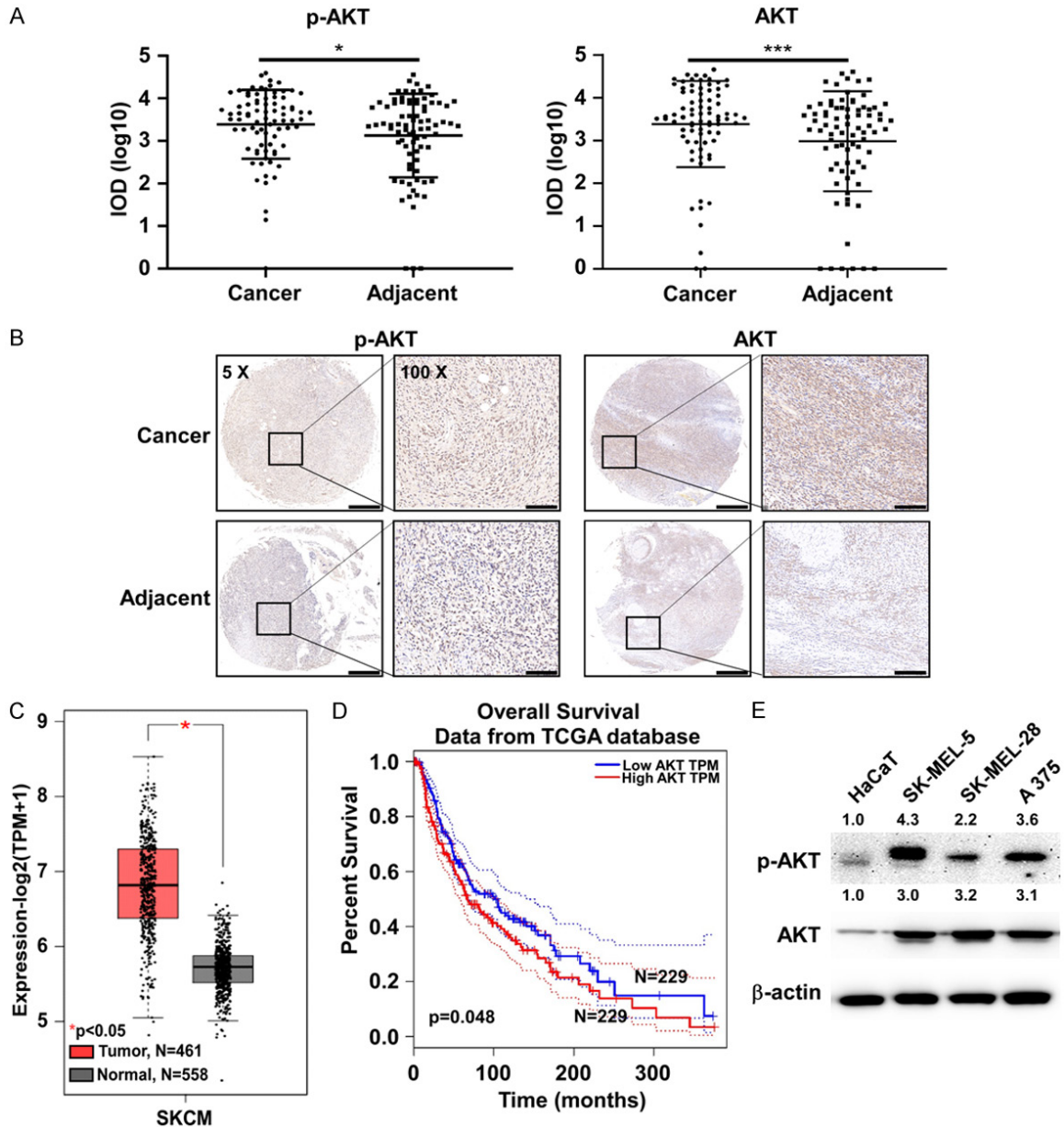
Figure 1. AKT expression in melanoma cell and patients versus that related to patient survival. A. The expression of phosphorylated AKT (Ser473) and total AKT was examined using immunohistochemical (IHC) analysis on a melanoma tumor tissue array. Data are shown on a log scale. *P < 0.05; ***P < 0.001 indicate a significant difference compared with adjacent tissues. B. Representative images of IHC staining on melanoma adjacent (n = 70), and cancer (n = 70) tissues, separately (5 × and 100 × magnification, Scale bars: 100 μm). C. The mRNA expression of AKT was evaluated in melanoma patients (data obtained from http://gepia.cancer-pku.cn/). D. Overall survival time of patients with high or low expression of AKT (data obtained from http://gepia.cancer-pku.cn/). E. The expression of AKT in melanoma cell lines evaluated using a Western blot assay and compared with normal skin cells.

CTD on the expression of apoptosis biomarkers by immunoblot. The immunoblot results indicated that the expression of apoptosis markers including p53, cleaved caspase-3, and Bax, were significantly increased; the anti-apoptotic protein Bcl-2 was markedly decreased (**Figure 3F**). These results suggest that CTD can reduce the growth of melanoma cells and induced apoptosis.

CTD suppresses migration and invasion in melanoma cells

Metastases is the primary cause of melanoma-related mortality. To investigate the role of CTD on migration and invasion in melanoma cells wound healing and transwell assay were performed. The results indicated that the migrated area was inhibited compare to the DMSO con-
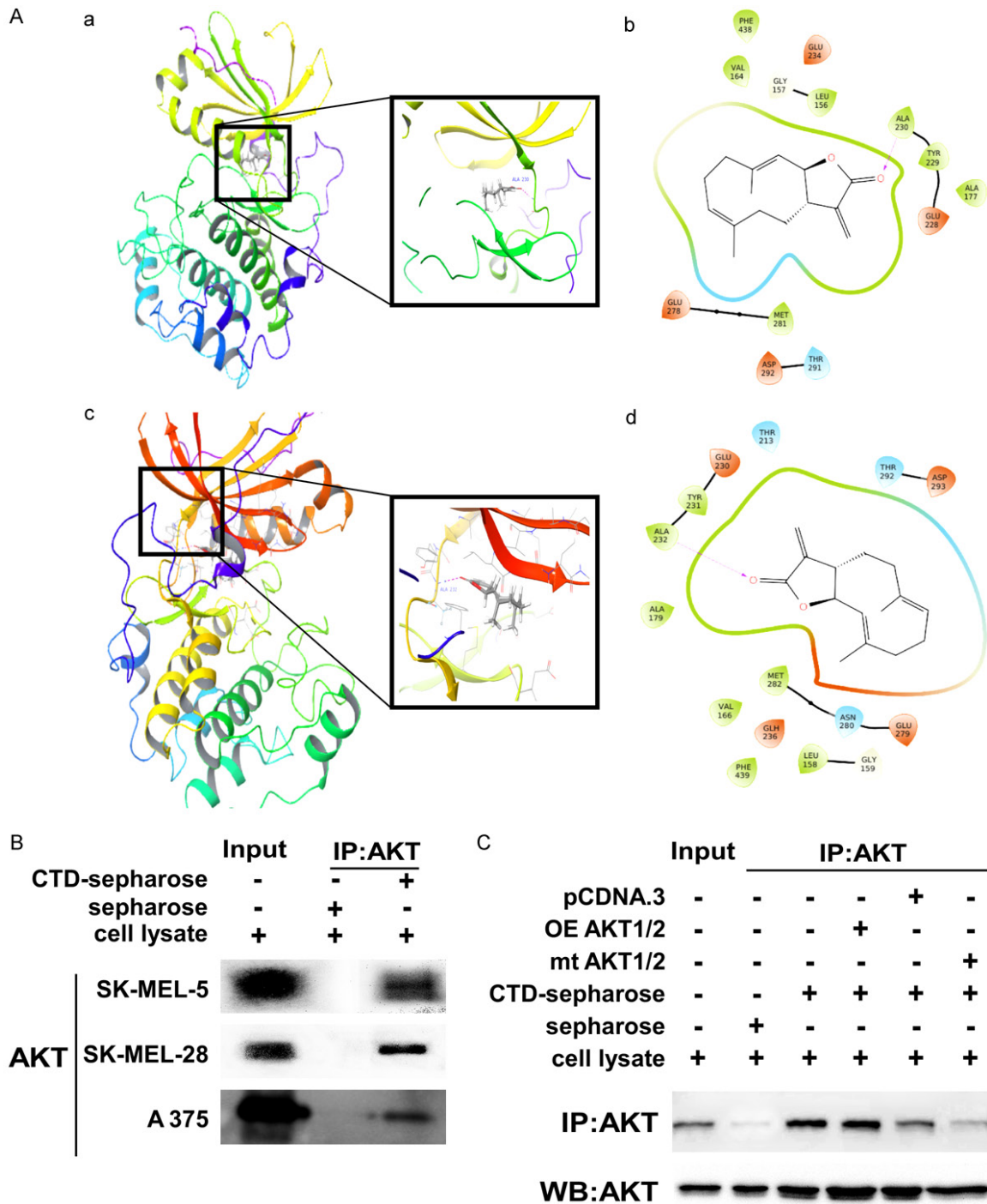
Figure 2. AKT is a target of CTD. (A) The computational docking model was conducted to predict the communication between CTD and AKT1 or AKT2: (a) CTD combines with AKT1; (b) Ligand interaction diagram of CTD and AKT1 conjugated; (c) CTD combines with AKT1; (d) Ligand interaction diagram of CTD and AKT1 conjugated. (B) The binding of CTD to AKT in melanoma cell lysates determined using sepharose 4B alone and costunolide-conjugated sepharose 4B beads. (C) Transfect plasmids of the mutant AKT1 and AKT2 into 293T cell after mutant the Ala site of AKT to confirm bonding capability between the CTD and AKT through pull-down assay.

trol group (**Figure 4A**). Furthermore, cell migration was analyzed through a Transwell assay. Similar to the results of the wound healing

assay, the Transwell suggested that CTD dramatically inhibited cell migration (**Figure 4B**, Supplementary Figure 2A). Moreover, we exam-
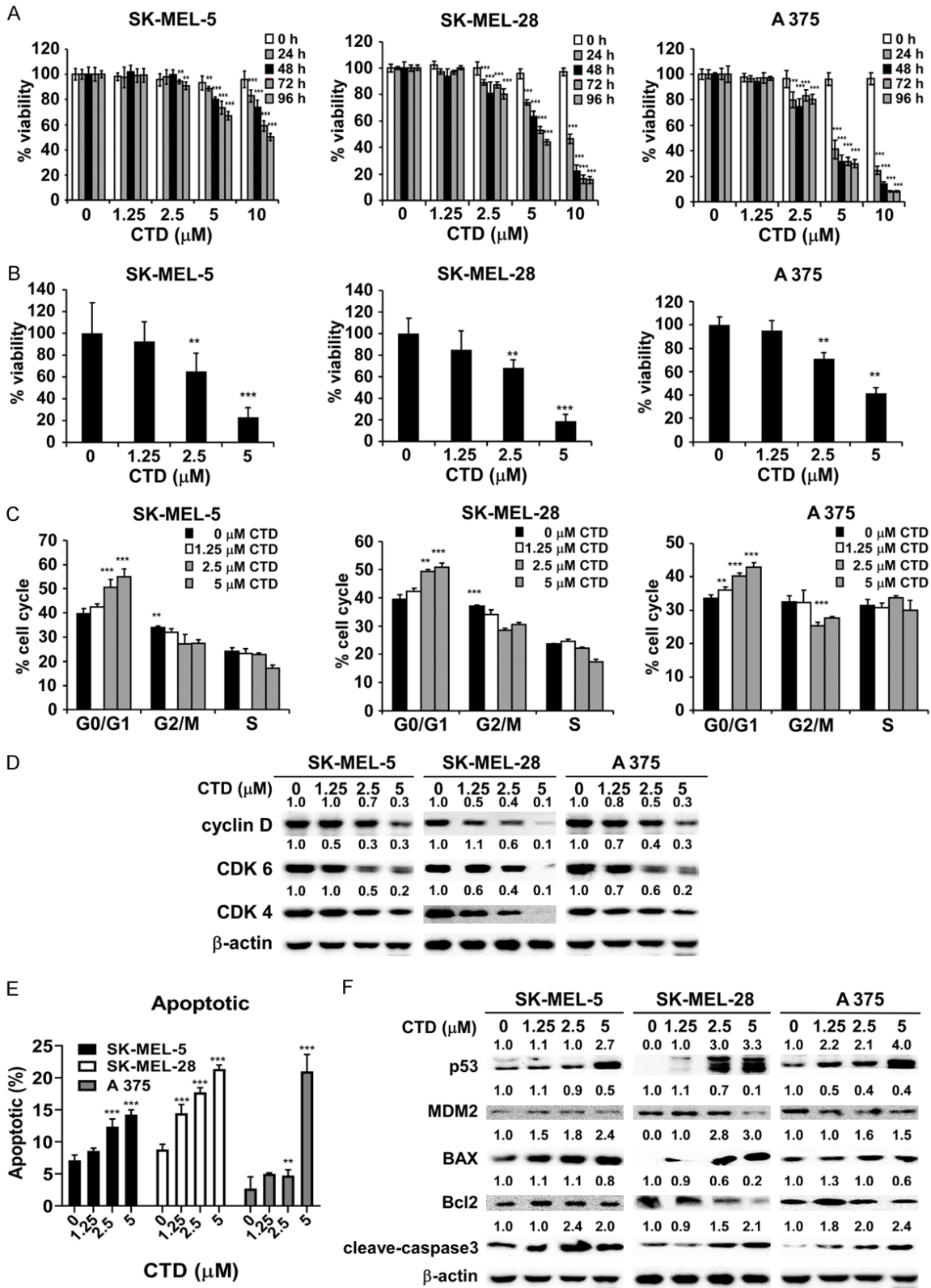
Figure 3. CTD suppresses the proliferation and trigger cell cycle arrest and apoptosis in melanoma. A. Cell proliferation of melanoma following CTD (0, 1.25, 2.5, and 5 μM) treatment was determined by MTT assay. B. Anchorage-independent cell growth assay was conducted to evaluate the effect of CTD on cell growth. C. CTD treatment induced cell cycle arrest at the G1 phase at 24 h. D. CTD effects on cyclinD1, CDK4, and CDK6 that makers of G1 phase. E.

CTD treatment triggered apoptosis at 24 hrs based on annexin V+/PI- gating. F. Apoptotic and anti-apoptotic protein markers were determined after CTD treatment using Western blot detection 24 hr post-treatment. Data are shown as means ± S.D. of values, *P < 0.05, **P < 0.01, ***P < 0.001 indicate a significant difference compare to control group. Three independent replicates were performed and were statistically analyzed.
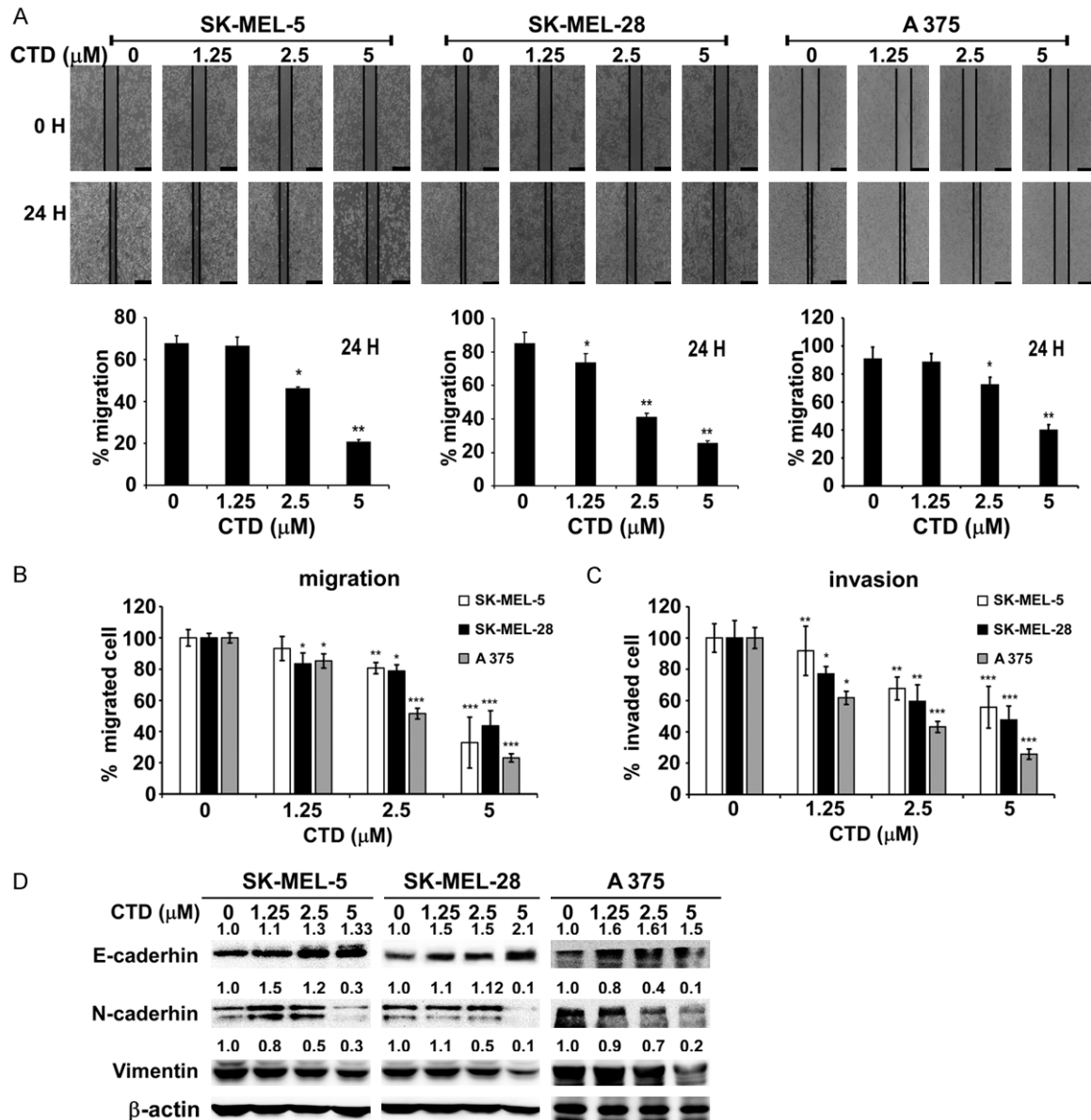
Figure 4. CTD suppresses the migration and invasion of melanoma cells. A. Treatment with CTD remarkably inhibited the migratory ability of the CRC cells in a wound healing assay. The representative images (Top: 50 × magnification, Scale bars: 100 μm) and the summary bar chart (Bottom) of the cells that migrated. B. Migration analysis of melanoma cells in the presences of CTD, or DMSO as the control, for 24 hours by transwell assay. C. Transwell analysis, with the Matrigel-coated membrane, of the effects of CTD treatment on melanoma cells. D. Protein expression of epithelial-mesenchymal transition markers were checked after CTD treatment when compared with the control. Data are shown as means ± S.D. of values from triplicate samples and similar results were obtained from three independent experiments. *P < 0.05, **P < 0.01, ***P < 0.001 indicate a significant difference compare to control group.

ined the effects of CTD on cell invasion through a matrigel-coated Transwell assay and found that CTD is a strong suppressor of melanoma invasion (**Figure 4C**, Supplementary Figure 2B). In addition, western blot results showed that E-cadherin expression was increased, while

N-cadherin and Vimentin expression were decreased in a concentration-dependent manner. The western blot results concur with the results of migration and invasion detection (**Figure 4D**). Collectively, CTD can effectively suppress melanoma cell migration.

CTD regulates AKT/mTOR/p70s6k signaling axis in melanoma cells

Given that AKT has been confirmed a target of CTD, the downstream of AKT signaling pathways were examined under the CTD treatment. The results showed that the AKT pathway was downregulated with CTD treatment through certain processes such as mTOR, p70S6K phosphorylation, and 4EBP1 phosphorylation (**Figure 5**). Furthermore, we also found that CTD could bind with BRAF (Supplementary Figure 3A). The expression of ERK1/2 was increased following CTD treatment as we checked the MAPK signaling pathway, suggesting that AKT/mTOR may be a primary pathway in melanoma treatment using CTD (Supplementary Figure 3B).

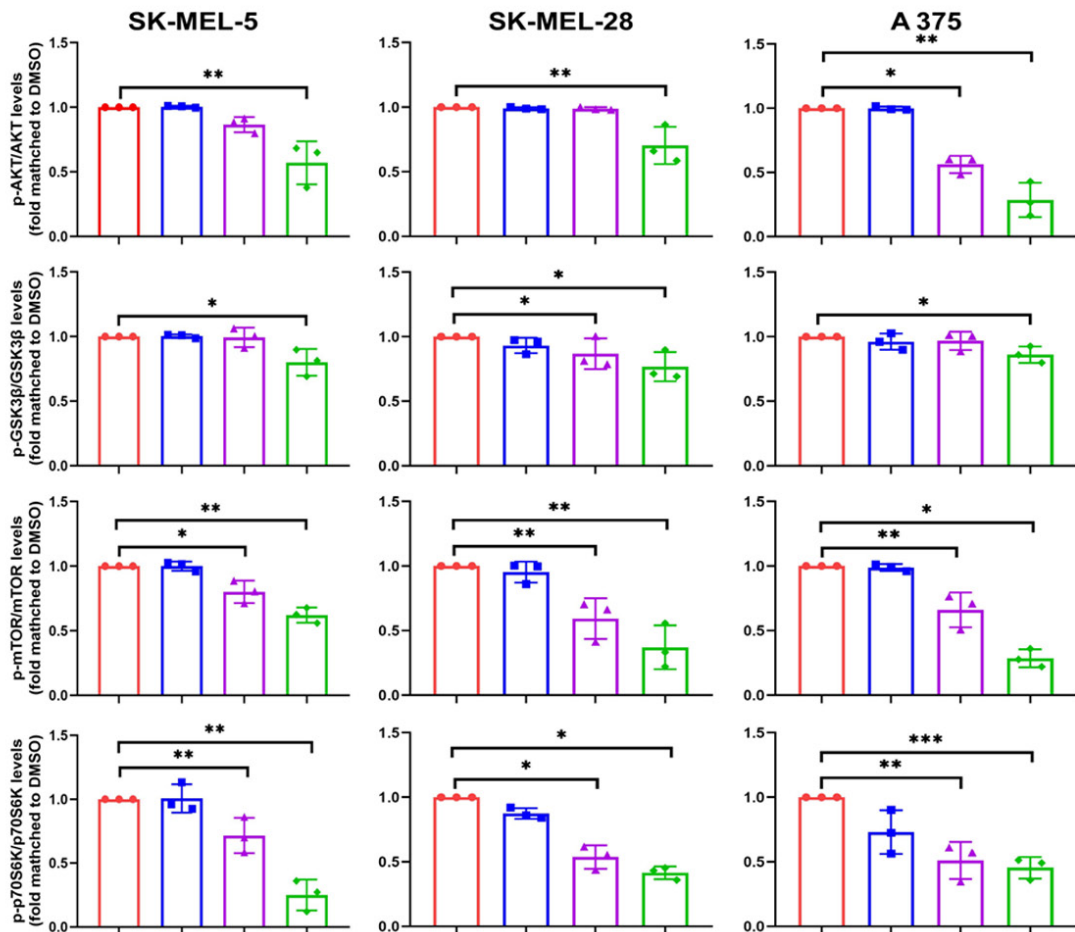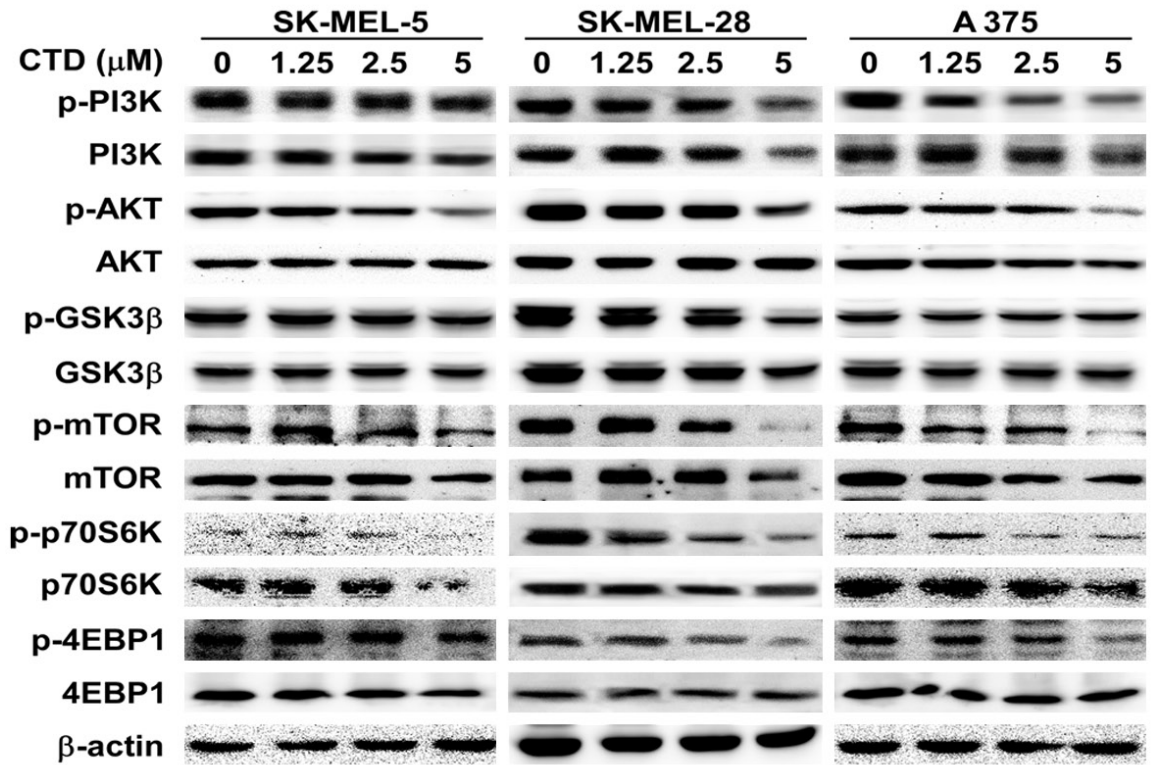*CTD suppresses the melanoma cells proliferation by targeting AKT*

To verify AKT expression inhibition that leads to the restrained growth of melanoma cells AKT knockdown cells were produced by infecting cells with virus particles containing shpLKO or shAKT1/2. Results of immunoblot revealed that the expression of AKT was reduced by shAKT in comparison with shpLKO (**Figure 6A**). MTT and anchorage-independent cell growth assays were conducted to examine cell proliferation and revealed that cell proliferation and colony formation was inhibited in AKT1/2 knockdown cell, compared with shpLKO-infected cells (**Figure 6B**, **6C**). However, CTD treatment failed to further inhibit colony formation in shAKT1/2 cells (**Figure 6C**, Supplementary Figure 4A), suggesting that AKT is a target of the CTD. Furthermore, the number of migrating and invading cells also decreased after AKT1/2 knockdown using the Transwell assay (**Figure 6D**, Supplementary Figure 4B). The western blot data showed a decrease in AKT downstream signaling after CTD treatment. However, there was no change in the knockdown of AKT1/2 cells that were simultaneously CTD-treated (**Figure 6E**). Moreover, AKT overexpres-

sion in melanoma cells showed that cell proliferation, migration, and invasion increased. AKT1/2 overexpressing cells showed more susceptible to CTD compared to mock cells (Supplementary Figure 5). Thus, AKT may considered a novel target of CTD in melanoma cells.

CTD inhibits tumor growth of cell-derived xenografts

Finally, xenograft models that built using SK-MEL-5 cells investigated the anti-tumor effects of CTD *in vivo*. Melanoma cells were implanted and then treatment with CTD at 5 mg/kg or 7.5 mg/kg. The results showed that CTD treatment effectively reduced tumor growth relative to the vehicle group without causing any change in mice body weight (**Figure 7A-C**). The immunohistochemical analysis showed that the CTD-treated groups showed decreased Ki-67, p-AKT, and p-p70S6K expression, compared with the vehicle-treated control (**Figure 7D**, **7E**). These results indicate that tumor volume and weight inhibition by CTD treatment is dependent on activation of AKT. To confirm the results of the *in vivo* model, we investigated the effects of CTD on AKT and its downstream signaling targets through western blot analysis of cell-derived xenograft (CDX) tumor tissue samples. The phosphorylation of p-mTOR and p-p70S6K, which are direct downstream proteins of AKT, was actively suppressed in the CTD-treated group (**Figure 7F**). Given that CTD drastically decreased the migration and invasive potential of melanoma cells *in vitro*, all major organs of the full necropsies were checked after the animals were sacrificed. We found that metastatic tumors appeared on the liver less frequently in treated mice than those in the control group (Supplementary Figure 6A). Moreover, the H&E staining results showed an appreciable decrease in the size and number of metastatic foci in the livers of CTD-treated mice, compared with that of vehicle-treated mice (Supplementary Figure 6B). The necropsy results indicate that CTD treatment significantly inhibited tumor metastasis *in vivo*. In addition, we also found that CTD downregulated the MAPK pathway *in vivo* (Supplementary Figure 6C). Collectively, combination with the *in vitro* study, these findings suggest that targeting AKT using CTD is an effective way to inhibit tumor growth and
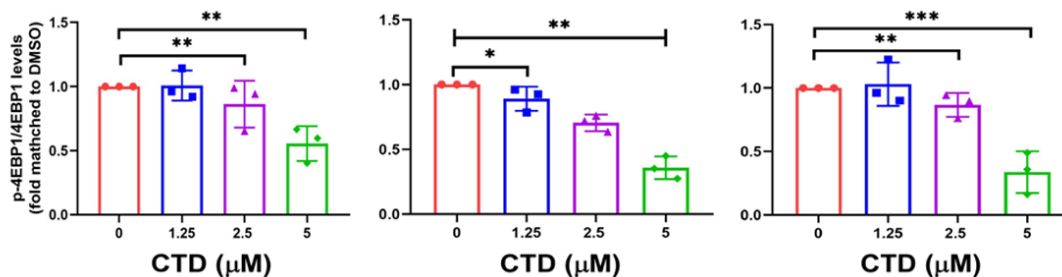
Figure 5. CTD suppresses the signaling pathway of AKT. The effects of CTD on AKT pathway and melanoma cells were examined by Western blot analysis. Cells were treated with CTD for 12 hours at various doses of 0, 1.25, 2.5, or 5 µM. Cells were collected and cell lysates were subjected to Western blotting.

metastases, which possibly acts by blocking the AKT signaling pathway.

Discussion

The aberrant expression and activity of the AKT signaling pathway proteins have been seen in biological processes such as metabolism, proliferation, apoptosis, and metastasis in several cancers, including melanoma [21, 36-40]. Recent studies have indicated that AKT was highly phosphorylated, or activated, in cancer tissues at different stages when compared with adjacent tissues in esophageal squamous and colon cancer [35, 39]. Additionally, AKT1/2 knockdown in cancer cells led to decreased colony formation. Therefore, AKT can be considered a therapeutic agent for treating malignant tumors. Several cancers are currently treated with AKT inhibitors including MK2206, GDC-0068, and GSK690693 [37]. However, some genetic mutations (BRAF, NRAS, AKT, and mTOR) exist in melanoma, and thus identifying new, more specific, and effective inhibitors that interrupt resistance pathways or those that can be combined with clinical drugs to improve the therapeutic efficacy is particularly important. Numerous phytomedicines exhibit melanoma inhibitory activities *in vitro* and *in vivo* [41]. In the present study, we investigated the chemotherapeutic activity of CTD against human melanoma.

Mechanistically, the anti-cancer effects of CTD are associated with the downregulation of STAT3, c-Myc, and nuclear factor-κB (NF-κB) that lead to cancer cell growth was inhibited and trigger apoptosis and cell cycle [42, 43]. However, the mechanisms underlying its chemo-preventive/therapeutic effects and direct

targets on melanoma remain unresolved. AKT pathway activation has been reported to play an essential role in the intracellular signaling pathway downstream of many non-melanoma and melanoma-related growth factor receptors [44]. In the present study, we identified the target of CTD and demonstrated that CTD is a potent AKT inhibitor of melanoma in both *in vitro* and *in vivo* (**Figures 3** and **6**). Our results, obtained using TCGA date and western blot analysis, show that AKT expression was more significant in melanoma when compared with other cancers and adjacent normal tissue. Our results also showed that AKT expression is associated with decreased patient survival time (**Figure 1**), suggesting that AKT expression is related to poor outcomes. Besides, metastasis dramatically impairs the successful treatment of advanced melanoma [45]. Our results indicate that CTD effectively inhibited the migration and invasion capabilities of melanoma cells (**Figure 4**), suggesting that inhibiting metastasis by targeting AKT may be an effective method in treating melanoma.

Our previous study showed that CTD could regulate MDM2-P53 by targeting AKT. To further confirm that AKT is a target of CTD, computational modeling illustrated how CTD interacts with AKT1 or AKT2. The modeling showed that Ala230 or Ala232 is the exclusive binding site in the backbone of AKT1 and AKT2. Furthermore, through a pull-down assay, we confirmed that CTD bound to AKT *in vitro* (**Figure 2A**, **2B**). Conversely, after a mutation in the Ala site of AKT, we found that the CTD bond to AKT was weaker when compared with the control group (**Figure 2C**). This strongly indicated that AKT is a target of CTD. Liu *et al.* (2019) reported the predictive docking model of xanthohumol and
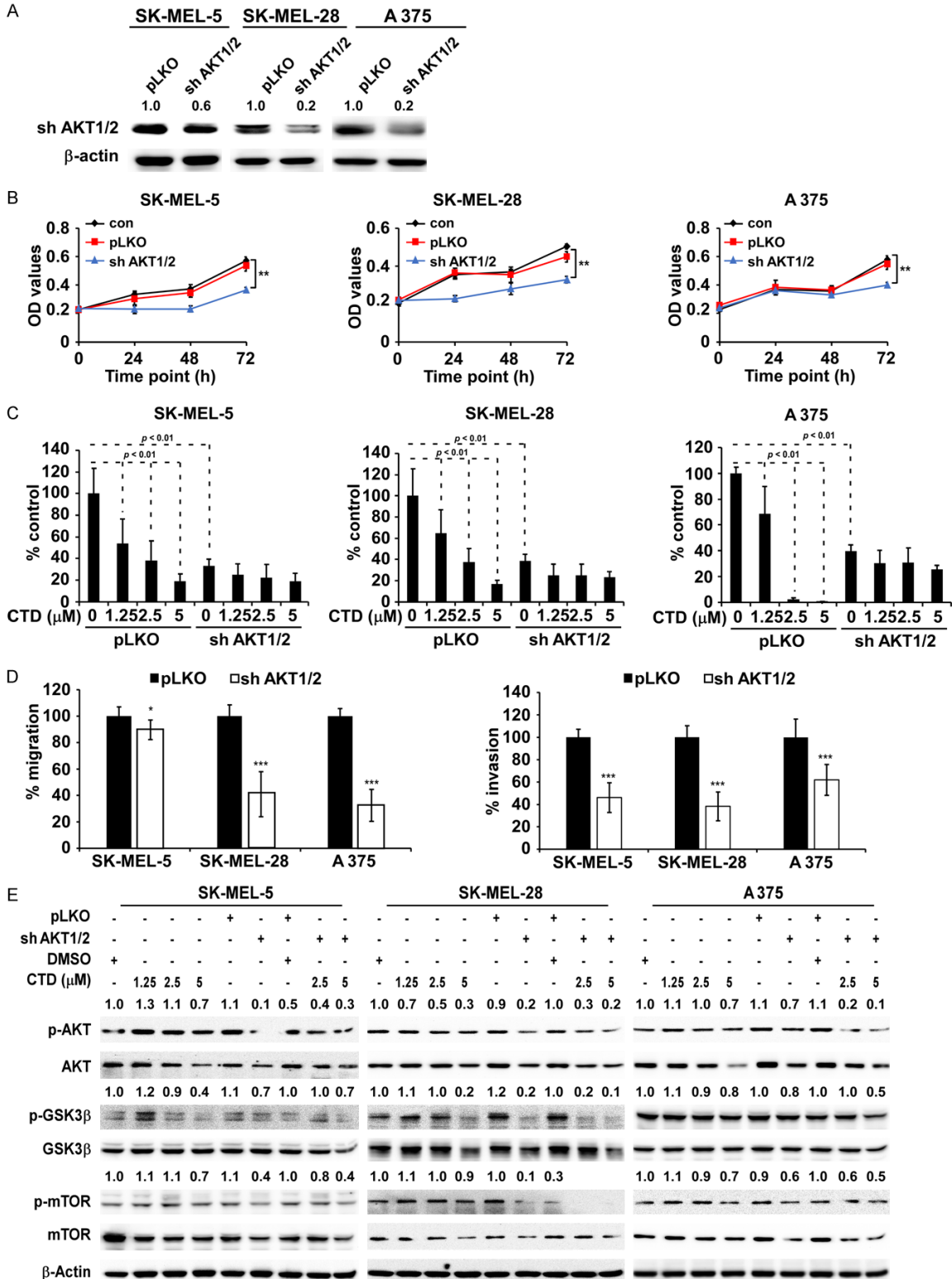
Figure 6. Effect of costunolide on AKT expression in melanoma cells. A. Expression of AKT in SK-MEL5, SK-MEL28, and A375 melanoma cells expressing pLKO or shRNA-AKT was evaluated. B. The cell proliferation of melanoma cell was evaluated after knockdown of AKT compared to the wild type. C. Anchorage-independent growth was assessed in SK-MEL5, SK-MEL28, and A375 melanoma cells expressing shRNA-pLKO or shRNA-AKT. D. Migration and invasion were assessed in SK-MEL5, SK-MEL28, and A375 melanoma cells expressing shRNA-pLKO or shRNA-AKT. Data are shown as means ± S.D. of three independent replicates. *P < 0.05, **P < 0.01, ***P < 0.001 indicate a significant difference compare to the control group. E. Western blots of the effects of costunolide treatment after knockdown AKT in melanoma compared with the shRNA-pLKO group.
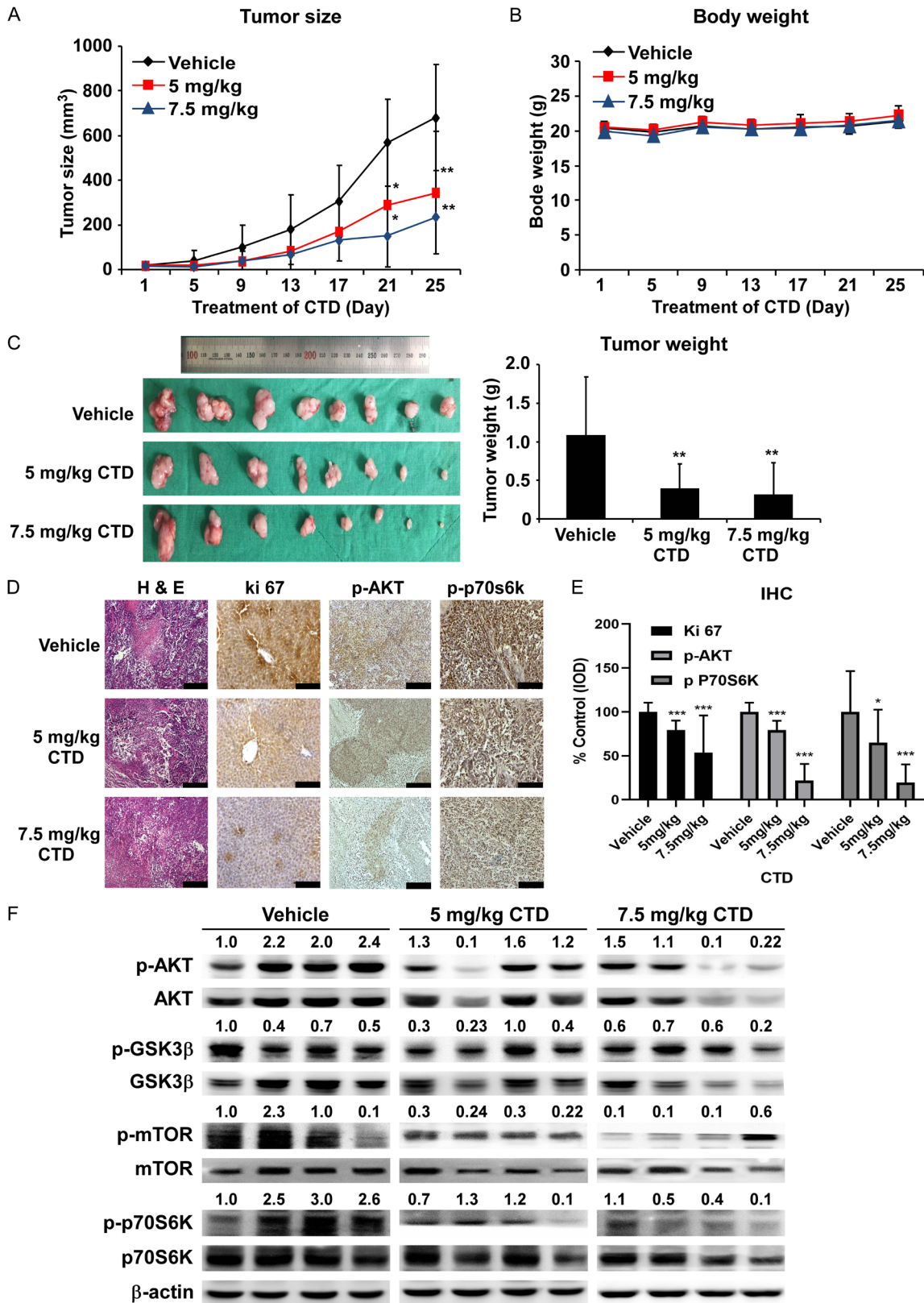
Figure 7. CTD inhibits mice tumor growth of xenografts model. Mice were divided into 3 groups (N = 8) to determine the effect of CTD on a melanoma cell-derived xenograft (CDX) tumor growth. The two treatment groups received 5 mg/kg and 7.5 mg/kg of CTD and the third group received only the vehicle. Mice were intraperitoneally adminis-

tered CTD or vehicle 3 times a week for 30 days. A. CTD inhibits melanoma growth. B. Body weights from treated or vehicle groups of mice were obtained every 4 days and showed that CTD has no effect on mouse body weight. C. Tumor weight decreased after CTD treatment compared to vehicle treatment. (Left: Representative photographs of tumors). D. The expression of Ki-67, p-AKT, and p-p70S6K were examined using immunohistochemical analysis (100 X magnification). E. Quantification of protein expression from IHC positive staining. F. CTD inhibits the expression of p-AKT and their downstream signaling proteins in CDX melanoma tumor tissues. All data are shown as mean values ± S.D. (*P < 0.05, **P < 0.01, ***P < 0.001) indicate a significant differences decrease in the volume of tumors from CTD-treated mice and Values are quantified from IHC staining and expressed as the treatment group compared with the vehicle-treated group.

AKT1/2 binding site, including Ala230 [40], and demonstrated that AKT downstream products, such as p70s6k, 4EBP1, were phosphorylated. PI3K/AKT/mTOR/P70S6K pathway is an important intracellular signaling pathway with respect to cell survival and death. Therefore, CTD may suppress melanoma growth through its effect on the AKT/mTOR pathway (**Figure 5**). Apart from this, CTD failed to suppress further colony formation after AKT1/2 knockdown (**Figure 6A-C**), which also supports the notion that CTD is a potential AKT inhibitor. Moreover, after AKT knockdown, the migration and invasion of melanoma cells decreased when compared with that in the control group (**Figure 6D**).

Given the constitutive activation of MEK-ERK pathway, p38, JNK have also been studied in relation to melanoma [11, 46, 47]. We extended the study to determine if CTD inhibited the activity of other proteins (Supplementary Figure 3A); the findings revealed that CTD could bind to BRAF in small amounts. However, the MAPK pathway is not consistent *in vivo* and *in vitro*, which is mainly manifested in ERK expression (Supplementary Figures 3B and 6C). Therefore, CTD seems to work well during these two stages of melanoma in relation to the AKT and MAPK/p38 pathways. However, prior studies have reported that the AKT and p38 MAPK/ERK1/2 cascades play essential roles in preventing endothelial cell death in melanoma under restrictive culture conditions [48]. Therefore, based on our findings and prior studies [49, 50], we postulate that the AKT pathway plays a central role in inhibiting melanoma growth.

The CDX mode helps us to understand the mechanism of pharmacologic effects on the tumor and is an essential tool in tumor research *in vivo*. Therefore, we also estimated the effects of CTD on the growth of melanoma CDX tumors in mice. The tumor volume and weight as well as the related immunohistochemical (IHC) bio-

marker staining after CTD treatment in the CTD-treated mice were significantly less when compared with the vehicle group (**Figure 7**). In summary, our findings indicated that AKT is a target of CTD, and it can decrease the viability of melanoma cells and reduce the growth of SK-MEL-5 human melanoma cells in a xenograft model in nude mice. All these results indicate that CTD is a potential AKT inhibitor that can aid in preventing or treating melanoma and that CTD is a potent chemo-preventive and chemotherapeutic compound that may possibly contribute to the treatment of melanoma patients in the future.

Acknowledgements

Disclosure of conflict of interest

None.

Address correspondence to: Myoung Ok Kim, Department of Animal Science and Biotechnology, Kyungpook National University, Sangju-si, Gyeongsang buk-do 37224, Republic of Korea. Tel: +82-01085893333; Fax: +82-545301229; E-mail: ok4325@knu.ac.kr; Zaeyoung Ryoo, School of Life Science, Kyungpook National University, Daegu, Republic of Korea. Tel: +82-053-950-7361; E-mail: jaewoong64@hanmail.net

References

[1] Chen WQ, Zheng RS, Baade PD, Zhang SW, Zeng HM, Bray F, Jemal A, Yu XQ and He J. Cancer statistics in China, 2015. CA Cancer J Clin 2016; 66: 115-132.

[2] Siegel RL, Miller KD and Jemal A. Cancer statistics, 2016. CA Cancer J Clin 2016; 66: 7-30.

[3] Beaver JA, Hazarika M, Mulkey F, Mushti S, Chen HY, He K, Sridhara R, Goldberg KB, Chuk

MK, Chi DC, Chang J, Barone A, Balasubramaniam S, Blumenthal GM, Keegan P, Pazdur R and Theoret MR. Patients with melanoma treated with an anti-PD-1 antibody beyond RECIST progression: a US Food and Drug Administration pooled analysis. Lancet Oncol 2018; 19: 229-239.

[4] Vilgelm AE, Saleh N, Shattuck-Brandt R, Riemenschneider K, Slesur L, Chen SC, Johnson CA, Yang JM, Blevins A, Yan C, Johnson DB, Al-Rohil RN, Halilovic E, Kauffmann RM, Kelley M, Ayers GD and Richmond A. MDM2 antagonists overcome intrinsic resistance to CDK4/6 inhibition by inducing p21. Sci Transl Med 2019; 11: eaav7171.

[5] Byron Y, Nott L and Shackleton M. Case report: acute tumour lysis syndrome following encorafenib and binimetinib for v600E metastatic melanoma with large intra-abdominal mass. Melanoma Res 2020; 30: 625-627.

[6] Girotti MR, Saturno G, Lorigan P and Marais R. No longer an untreatable disease: how targeted and immunotherapies have changed the management of melanoma patients. Mol Oncol 2014; 8: 1140-1158.

[7] Bhatia S, Tykodi SS and Thompson JA. Treatment of metastatic melanoma: an overview. Oncology (Williston Park) 2009; 23: 488-496.

[8] Gide TN, Wilmott JS, Scolyer RA and Long GV. Primary and acquired resistance to immune checkpoint inhibitors in metastatic melanoma. Clin Cancer Res 2018; 24: 1260-1270.

[9] Russo I, Zorzetto L, Frigo AC, Sileni VC and Alaibac M. A comparative study of the cutaneous side effects between BRAF monotherapy and BRAF/MEK inhibitor combination therapy in patients with advanced melanoma: a single-centre experience. Eur J Dermatol 2017; 27: 482-486.

[10] McKean M, Oba J, Ma JS, Roth KG, Wang WL, Macedo MP, Carapeto FCL, Haydu LE, Siroy AE, Vo P, Hong DS, Eterovic AK, Patel KP, Bassett RL, Grimm EA, Lazar AJ and Woodman SE. Tyrosine kinase inhibitor and immune checkpoint inhibitor responses in KIT-mutant metastatic melanoma. J Invest Dermatol 2019; 139: 728-731.

[11] Savoia P, Fava P, Casoni F and Cremona O. Targeting the ERK signaling pathway in melanoma. Int J Mol Sci 2019; 20: 1483.

[12] Cheng YB, Zhang GH and Li G. Targeting MAPK pathway in melanoma therapy. Cancer Metastasis Rev 2013; 32: 567-584.

[13] Pollock PM, Harper UL, Hansen KS, Yudt LM, Stark M, Robbins CM, Moses TY, Hostetter G, Wagner U, Kakareka J, Salem G, Pohida T, Heenan P, Duray P, Kallioniemi O, Hayward NK, Trent JM and Meltzer PS. High frequency of BRAF mutations in nevi. Nat Genet 2003; 33: 19-20.

[14] Poynter JN, Elder JT, Fullen DR, Nair RP, Soengas MS, Johnson TM, Redman B, Thomas NE and Gruber SB. BRAF and NRAS mutations in melanoma and melanocytic nevi. Melanoma Res 2006; 16: 267-273.

[15] Nazarian R, Shi HB, Wang Q, Kong XJ, Koya RC, Lee H, Chen ZG, Lee MK, Attar N, Sazegar H, Chodon T, Nelson SF, McArthur G, Sosman JA, Ribas A and Lo RS. Melanomas acquire resistance toB-RAF(V600E) inhibition by RTK or N-RAS upregulation. Nature 2010; 468: 973-U377.

[16] Villanueva J, Vultur A, Lee JT, Somasundaram R, Fukunaga-Kalabis M, Cipolla AK, Wubbenhorst B, Xu XW, Gimotty PA, Kee D, Santiago-Walker AE, Letrero R, D'Andrea K, Pushparajan A, Hayden JE, Brown KD, Laquerre S, McArthur GA, Sosman JA, Nathanson KL and Herlyn M. Acquired resistance to BRAF inhibitors mediated by a RAF kinase switch in melanoma can be overcome by cotargeting MEK and IGF-1R/PI3K. Cancer Cell 2010; 18: 683-695.

[17] Segrelles C, Ruiz S, Perez P, Murga C, Santos M, Budunova IV, Martinez J, Larcher F, Slaga TJ, Gutkind JS, Jorcano JL and Paramio JM. Functional roles of Akt signaling in mouse skin tumorigenesis. Oncogene 2002; 21: 53-64.

[18] Jazirehi AR, Wenn PB and Damavand M. Therapeutic implications of targeting the PI3Kinase/AKT/mTOR signaling module in melanoma therapy. Am J Cancer Res 2012; 2: 178-191.

[19] Soares CD, Borges CF, Sena M, de Almeida OP, Stelini RF, Cintra ML, Graner E, Zecchin KG and Jorge J. Prognostic significance of cyclooxygenase 2 and phosphorylated Akt1 overexpression in primary nonmetastatic and metastatic cutaneous melanomas. Melanoma Res 2017; 27: 448-456.

[20] Cho JH, Robinson JP, Arave RA, Burnett WJ, Kircher DA, Chen G, Davies MA, Grossmann AH, VanBrocklin MW, McMahon M and Holmen SL. AKT1 activation promotes development of melanoma metastases. Cell Rep 2015; 13: 898-905.

[21] Kircher DA, Trombetti KA, Silvis MR, Parkman GL, Fischer GM, Angel SN, Stehn CM, Strain SC, Grossmann AH, Duffy KL, Boucher KM, McMahon M, Davies MA, Mendoza MC, VanBrocklin MW and Holmen SL. AKT1(E17K) activates focal adhesion kinase and promotes melanoma brain metastasis. Mol Cancer Res 2019; 17: 1787-1800.

[22] Grottke A, Ewald F, Lange T, Norz D, Herzberger C, Bach J, Grabinski N, Graser L, Hoppner F, Nashan B, Schumacher U and Jucker M. Downregulation of AKT3 increases migration and

metastasis in triple negative breast cancer cells by upregulating S100A4. PLoS One 2016; 11: e0146370.

[23] Shi HB, Hong AY, Kong XJ, Koya RC, Song CY, Moriceau G, Hugo W, Yu CC, Ng C, Chodon T, Scolyer RA, Kefford RF, Ribas A, Long GV and Lo RS. A novel AKT1 mutant amplifies an adaptive melanoma response to BRAF inhibition. Cancer Discov 2014; 4: 69-79.

[24] Irvine M, Stewart A, Pedersen B, Boyd S, Kefford R and Rizos H. Oncogenic PI3K/AKT promotes the step-wise evolution of combination BRAF/MEK inhibitor resistance in melanoma. Oncogenesis 2018; 7: 72.

[25] Erdmann S, Seidel D, Jahnke HG, Eichler M, Simon JC and Robitzki AA. Induced cross-resistance of BRAF(V600E) melanoma cells to standard chemotherapeutic dacarbazine after chronic PLX4032 treatment. Sci Rep 2019; 9: 30.

[26] Niessner H, Forschner A, Klumpp B, Honegger JB, Witte M, Bornemann A, Dummer R, Adam A, Bauer J, Tabatabai G, Flaherty K, Beck D, Leiter U, Mauch C, Rosch A, Weide B, Eigentler T, Schadendorf D, Garbe C, Kulms D, Quintanilla-Martinez L and Meier F. Targeting hyperactivation of the AKT survival pathway to overcome therapy resistance of melanoma brain metastases. Exp Dermatol 2013; 22: E38-E38.

[27] Davies MA. The role of the PI3K-AKT pathway in melanoma. Cancer J 2012; 18: 142-147.

[28] Hua PY, Sun M, Zhang GX, Zhang YF, Song G, Liu ZY, Li X, Zhang XY and Li BJ. Costunolide induces apoptosis through generation of ROS and activation of P53 in human esophageal cancer Eca-109 cells. J Biochem Mol Toxicol 2016; 30: 462-9.

[29] Hua PY, Zhang GX, Zhang YF, Sun M, Cui RJ, Li X, Li BJ and Zhang XY. Costunolide induces G1/S phase arrest and activates mitochondrial-mediated apoptotic pathways in SK-MES 1 human lung squamous carcinoma cells. Oncol Lett 2016; 11: 2780-2786.

[30] Mao JX, Yi M, Tao YY, Huang YS and Chen M. Costunolide isolated from Vladimiria souliei inhibits the proliferation and induces the apoptosis of HepG2 cells. Mol Med Rep 2019; 19: 1372-1379.

[31] Zhuge W, Chen R, Vladimir K, Dong X, Zia K, Sun X, Dai X, Bao M, Shen X and Liang G. Costunolide specifically binds and inhibits thioredoxin reductase 1 to induce apoptosis in colon cancer. Cancer Lett 2018; 412: 46-58.

[32] Pan Y, Li J, Zhang Y, Wang N, Liang H, Liu Y, Zhang CY, Zen K and Gu H. Slug-upregulated miR-221 promotes breast cancer progression through suppressing E-cadherin expression. Sci Rep 2016; 6: 25798.

[33] Berman HM, Westbrook J, Feng Z, Gilliland G, Bhat TN, Weissig H, Shindyalov IN and Bourne PE. The protein data bank. Nucleic Acids Res 2000; 28: 235-242.

[34] Zhao R, Huang H, Choi BY, Liu XJ, Zhang M, Zhou SL, Song MQ, Yin FX, Chen HY, Shim JH, Bode AM, Dong ZG and Lee MH. Cell growth inhibition by 3-deoxysappanchalcone is mediated by directly targeting the TOPK signaling pathway in colon cancer. Phytomedicine 2019; 61: 152813.

[35] Song MQ, Liu XJ, Liu KD, Zhao R, Huang H, Shi YY, Zhang M, Zhou SL, Xie H, Chen HY, Li Y, Zheng Y, Wu Q, Liu FF, Li EM, Bode AM, Dong ZG and Lee MH. Targeting AKT with oridonin inhibits growth of esophageal squamous cell carcinoma in vitro and patient-derived xenografts in vivo. Mol Cancer Ther 2018; 17: 1540-1553.

[36] Madhunapantula SV, Mosca PJ and Robertson GP. The Akt signaling pathway an emerging therapeutic target in malignant melanoma. Cancer Biol Ther 2011; 12: 1032-49.

[37] Song MQ, Bode AM, Dong ZG and Lee MH. AKT as a therapeutic target for cancer. Cancer Res 2019; 79: 1019-1031.

[38] Kim MO, Lee MH, Oi N, Kim SH, Bae KB, Huang ZN, Kim DJ, Reddy K, Lee SY, Park SJ, Kim JY, Xie H, Kundu JK, Ryoo ZY, Bode AM, Surh YJ and Dong Z. [6]-Shogaol inhibits growth and induces apoptosis of non-small cell lung cancer cells by directly regulating Akt1/2. Carcinogenesis 2014; 35: 683-691.

[39] Suman S, Das TP, Sirimulla S, Alatassi H, Ankem MK and Damodaran C. Withaferin-A suppress AKT induced tumor growth in colorectal cancer cells. Oncotarget 2016; 7: 13854-13864.

[40] Liu X, Song M, Wang P, Zhao R, Chen H, Zhang M, Shi Y, Liu K, Liu F, Yang R, Li E, Bode AM, Dong Z and Lee MH. Targeted therapy of the AKT kinase inhibits esophageal squamous cell carcinoma growth in vitro and in vivo. Int J Cancer 2019; 145: 1007-1019.

[41] Hwang SY, Chae JI, Kwak AW, Lee MH and Shim JH. Alternative options for skin cancer therapy via regulation of AKT and related signaling pathways. Int J Mol Sci 2020; 21: 6869.

[42] Jin X, Wang C and Wang L. Costunolide inhibits osteosarcoma growth and metastasis via suppressing STAT3 signal pathway. Biomed Pharmacother 2019; 121: 109659.

[43] Peng ZX, Wang Y, Fan JH, Lin XJ, Liu CY, Xu Y, Ji WD, Yan C and Su CQ. Costunolide and dehydrocostuslactone combination treatment inhibit breast cancer by inducing cell cycle arrest and apoptosis through c-Myc/p53 and AKT/14-3-3 pathway. Sci Rep 2017; 7: 41254.

[44] Crowell JA, Steele VE and Fay JR. Targeting the AKT protein kinase for cancer chemoprevention. Mol Cancer Ther 2007; 6: 2139-2148.

[45] Liu QH and Ma LS. Knockdown of thrombospondin 2 inhibits metastasis through modulation of PI3K signaling pathway in uveal melanoma cell line M23. Eur Rev Med Pharmacol Sci 2018; 22: 6230-6238.

[46] Ma LM, Xu Y, Wei ZL, Xin G, Xing ZH, Niu H and Huang W. Deoxyarbutin displays antitumour activity against melanoma in vitro and in vivo through a p38-mediated mitochondria associated apoptotic pathway. Sci Rep 2017; 7: 7197.

[47] Han YH, Mun JG, Jeon HD, Park J, Kee JY and Hong SH. Gomisin A ameliorates metastatic melanoma by inhibiting AMPK and ERK/JNK-mediated cell survival and metastatic phenotypes. Phytomedicine 2020; 68: 153147.

[48] Das AM, Pescatori M, Vermeulen CE, Rens JA, Seynhaeve AL, Koning GA, Eggermont AM and Ten Hagen TL. Melanomas prevent endothelial cell death under restrictive culture conditions by signaling through AKT and p38 MAPK/ ERK-1/2 cascades. Oncoimmunology 2016; 5: e1219826.

[49] Jazirehi AR, Wenn PB and Damavand M. Therapeutic implications of targeting the PI3Kinase/ AKT/mTOR signaling module in melanoma therapy. Am J Cancer Res 2012; 2: 178-191.

[50] Madhunapantula SV and Robertson GP. Therapeutic implications of targeting AKT signaling in melanoma. Enzyme Res 2011; 2011: 327923.
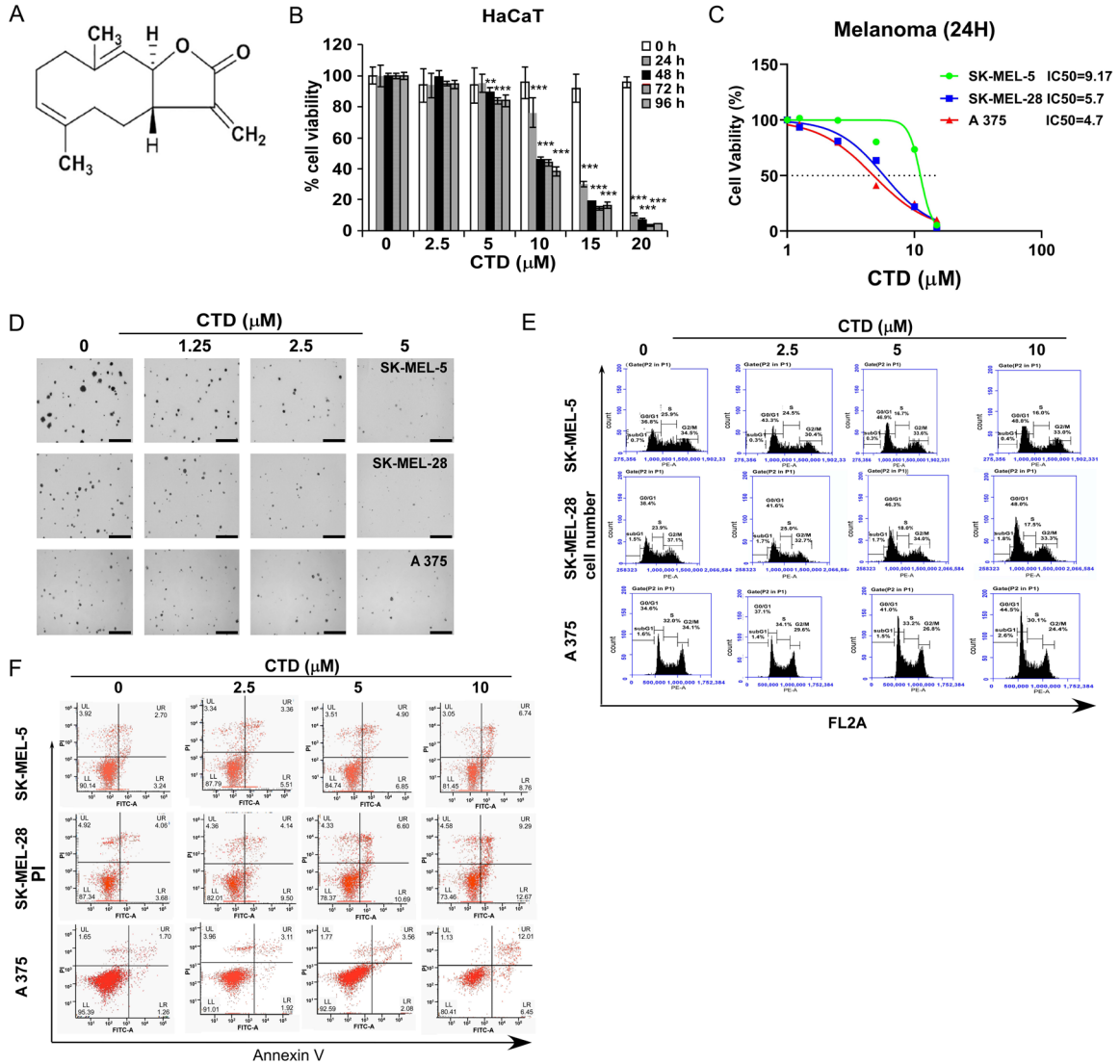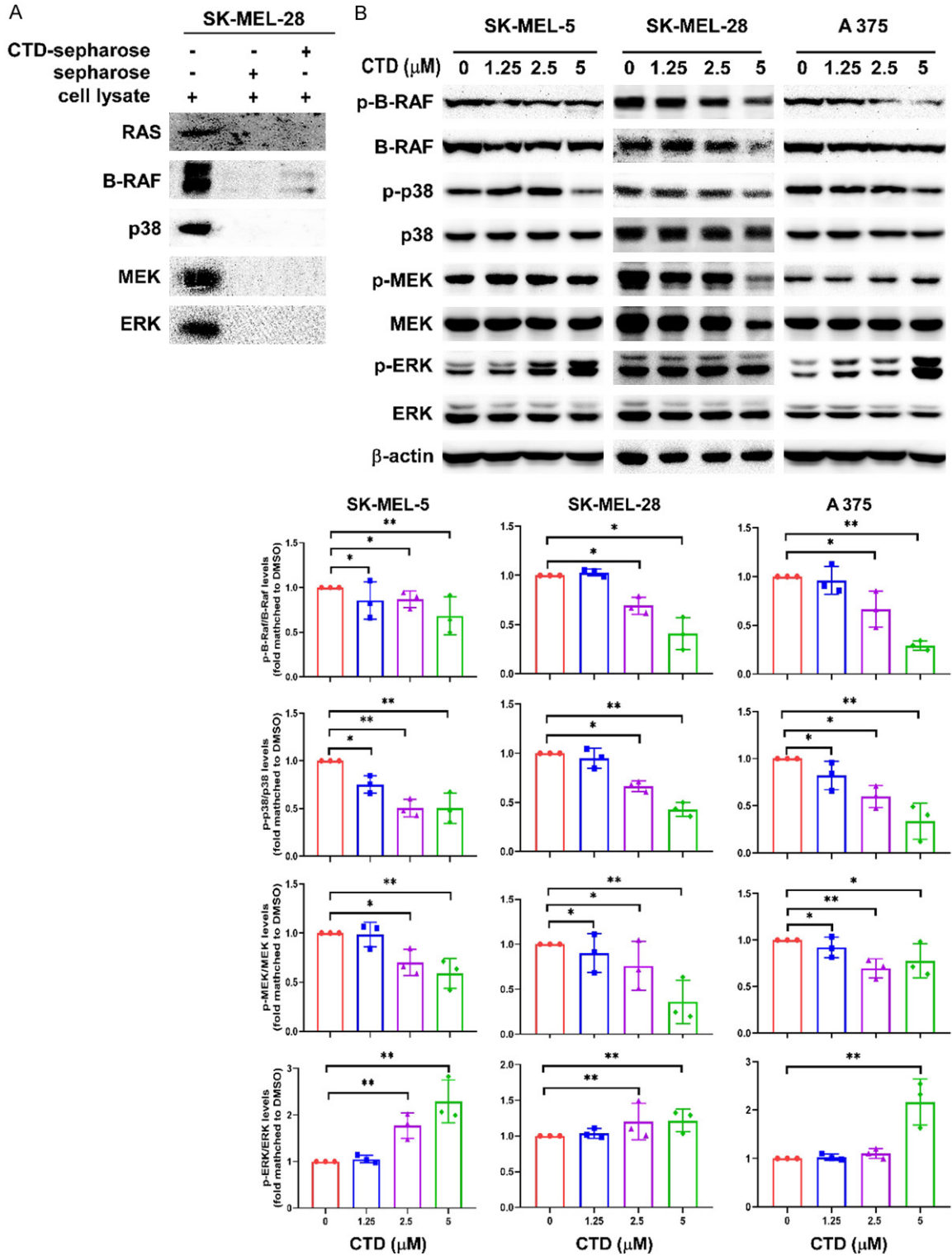
Supplementary Figure 1. Effects of Costunolide on cell proliferation, cell cycle, and apoptosis. A. Chemical structure of Costunolide. B. Cytotoxicity of Costunolide on normal HaCaT skin cells were estimated through MTT assay. The cells were treated with 0, 1.25, 2.5, or 5 μM Costunolide for different periods. C. IC50 concentration was detect on three melanoma cells. D. Corresponding images of anchorage-independent cell growth (5 × magnification, Scale bars: 100 μm). E. Plots indicating cell cycle distribution after administration of different Costunolide concentrations of (0, 1.25, 2.5, or 5 μM) to melanoma cells. F. Plots of apoptotic cell populations after administration of different Costunolide concentrations (0, 1.25, 2.5, or 5 μM) to melanoma cells.
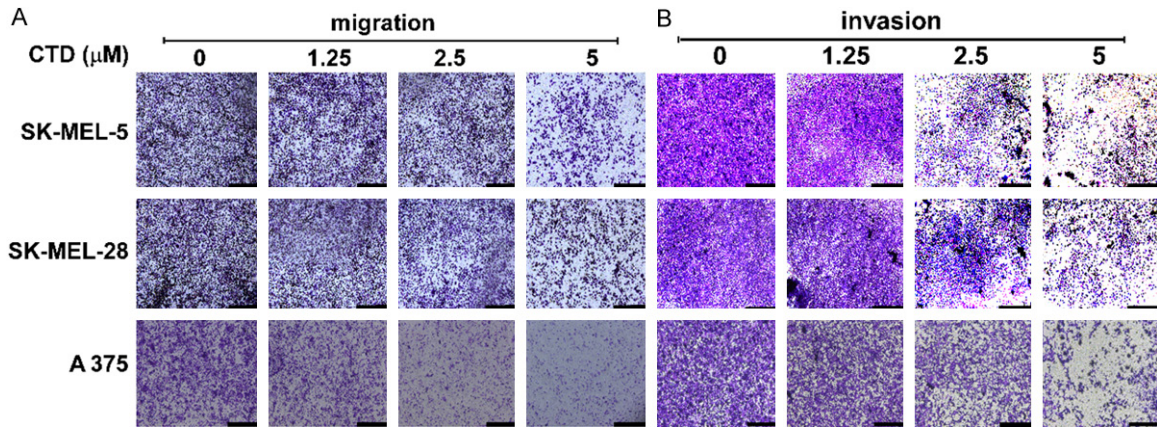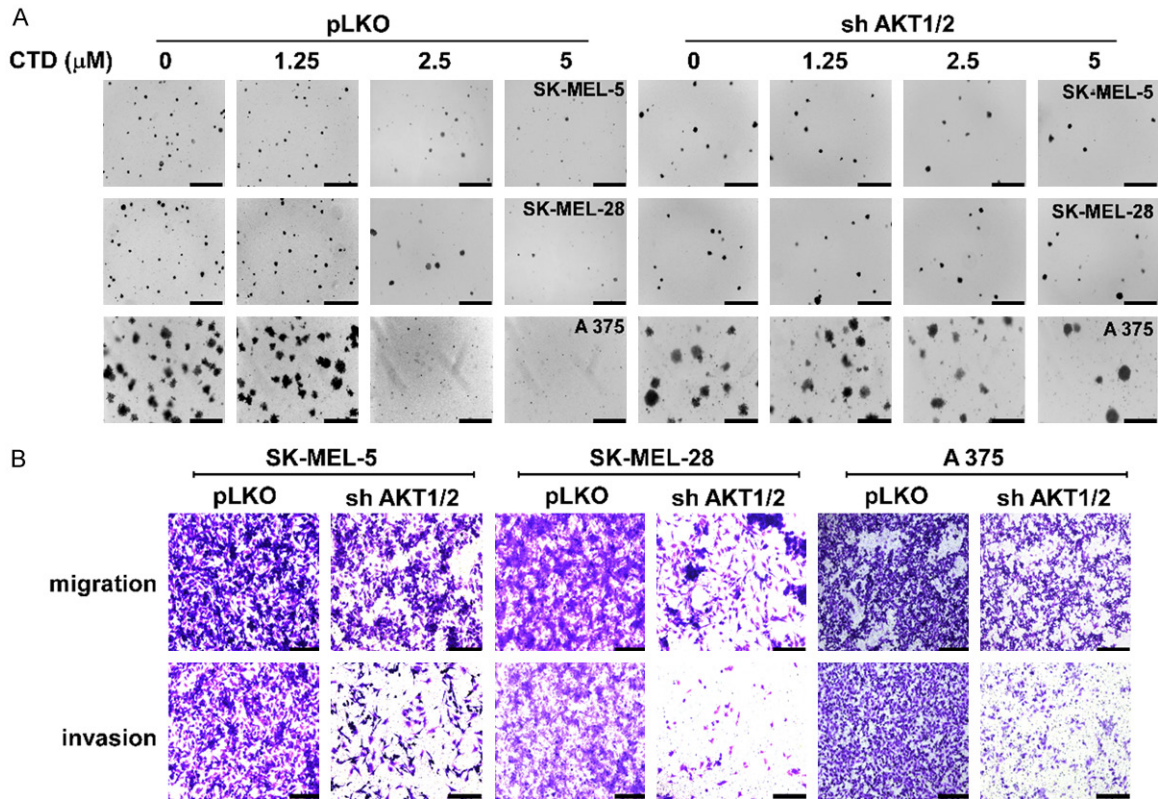
Supplementary Figure 2. Effects of Costunolide on melanoma cell migration and invasion. A. Representative photographs of migration after administration of different Costunolide concentrations to melanoma cells (5 × magnification, Scale bars: 100 μm). B. Representative photographs of invasion after administration of different Costunolide concentrations to melanoma cells (5 × magnification, Scale bars: 100 μm).

Supplementary Figure 3. The potential target of Costunolide and the associated pathways in melanoma. A. Costunolide binds to proliferation-related protein in a melanoma cell lysate. B. Western blot of the p-MEK1, p-ERK1/2 (T202/Y204), p-MEK, MEK, p-p38, and p38 proteins in melanoma cells after treatment with Costunolide for 12 h.
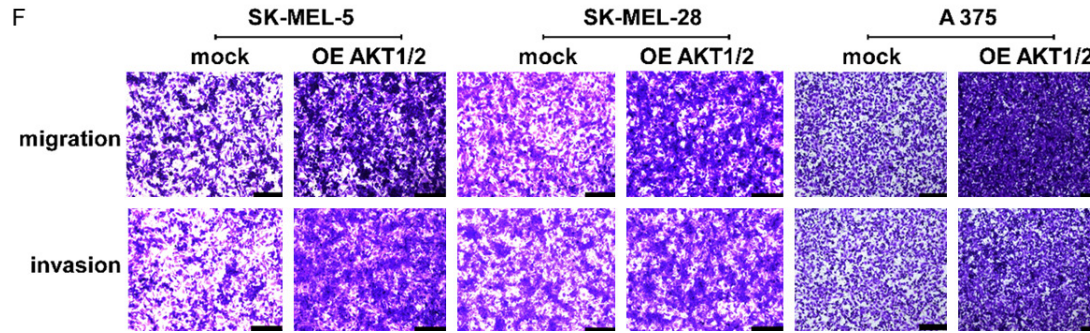
Supplementary Figure 4. Colony formation, migration, and invasion in melanoma cells after AKT1/2 knockdown. A. Representative colony pictures after AKT1/2 knockdown with or without Costunolide treatment (5 × magnification, Scale bars: 100 μm). B. Representative photographs of migration and invasion after AKT1/2 knockdown (10 × magnification, Scale bars: 100 μm).

A

B

C

D

E
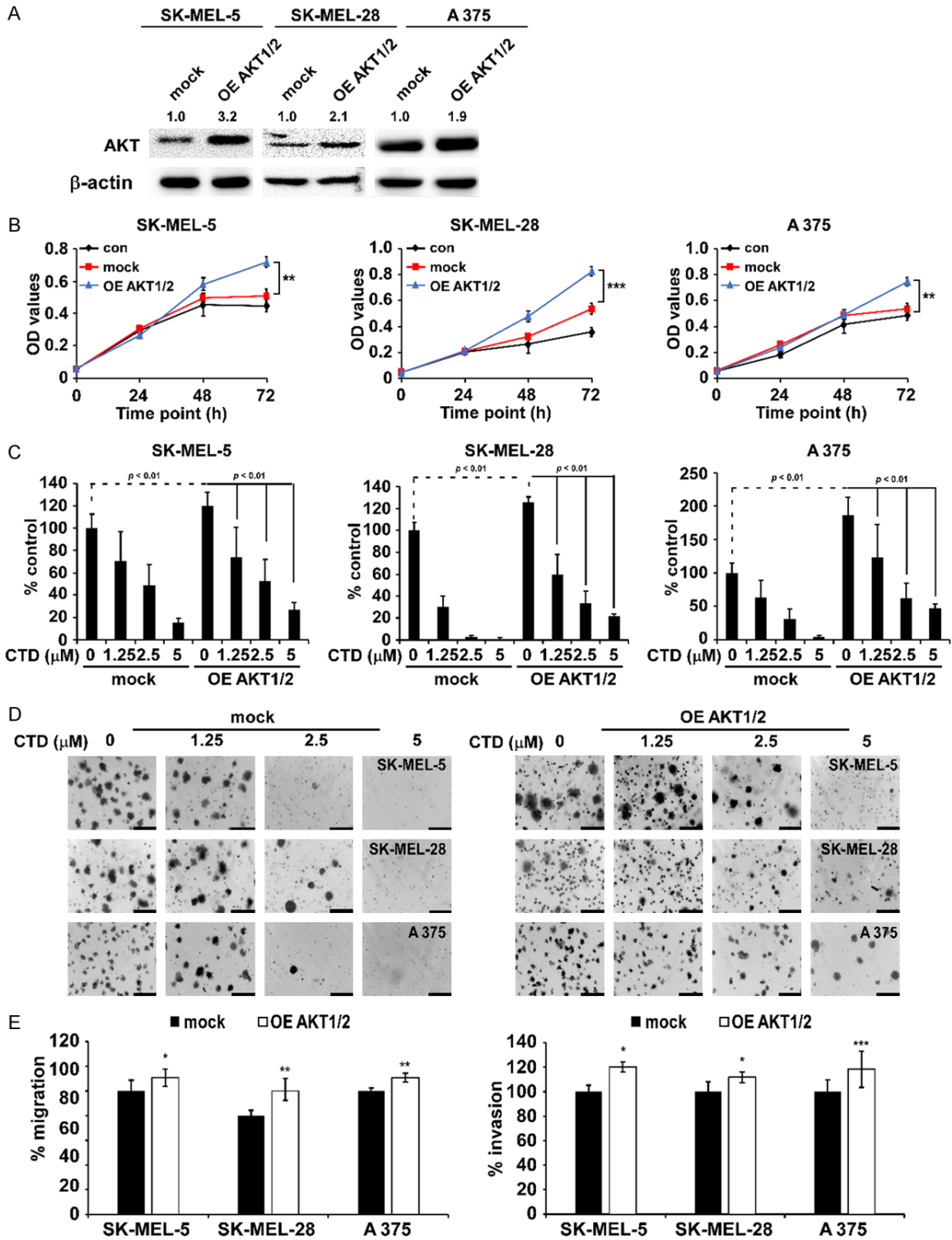
Supplementary Figure 5. Effects of AKT overexpression in melanoma cells. A. Western blotting analysis of AKT expression in melanoma cells with AKT1/2 overexpression. B. Growth curve of indicated stable AKT-overexpressing melanoma cells detected using a CCK-8 for cell proliferation assay (n = 6 per group) at 0, 24, 48, and 72 h. C. Colony formation was examined after followed CTD treatment in expressing mock or AKT1/2 cells by soft agar assay. D. Representative images of anchorage-independent cell growth shown after AKT1/2 overexpression (5 × magnification, Scale bars: 100 μm). E. Summary bar chart of cell migration through a membrane or invasion through a Matrigel-coated membrane. F. Representative photographs of migration and invasion after AKT1/2 overexpression (10 × magnification, Scale bars: 100 μm). All data are shown as mean values ± S.D., (*$P < 0.05$, **$P < 0.01$, and ***$P < 0.001$) indicate a significant difference in decreased proliferation, colony number, and cell migration and invasion, compared with the corresponding control.
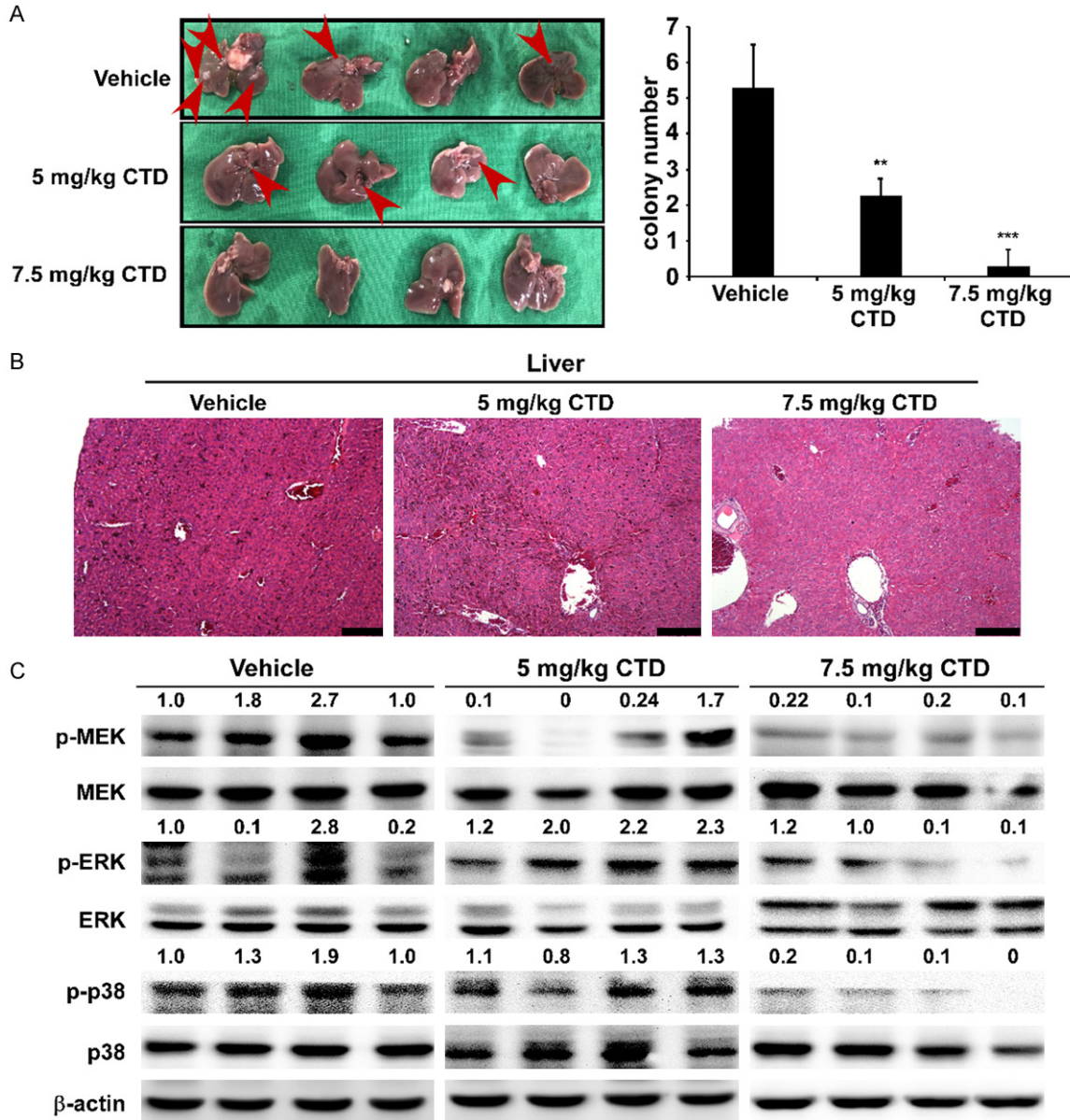
Supplementary Figure 6. The effect of Costunolide on tumor growth and metastasis in nude mice, and MAPK pathway was examined. A. SK-MEL-5 was intravenously injected into nude mice via the subcutaneous injection. Left, representative images of the excised liver after 4 weeks of injection (arrows indicate metastatic nodules). Right, the graph showing the number of surface metastatic foci in the liver. Data are shown as means ± S.D. (*P < 0.05, **P < 0.01, and ***P < 0.001) indicate a significant difference, compared with the corresponding control. B. Liver metastases in each mouse were confirmed by hematoxylin and eosin staining (5 × magnification, Scale bars: 100 μm). C. Western blot of the p-MEK1, p-ERK1/2 (T202/Y204), and p-p38 proteins in xenograft tissues.